THE ASTROPHYSICAL JOURNAL, 431:826–835, 1994 August 20

SPECTRAL VARIATIONS IN THE LOW-MASS X-RAY BINARY 4U 0614+09

K. P. SINGH AND K. M. V. APPARAO
Tata Institute of Fundamental Research, Bombay 400 005, India
Received 1993 December 2; accepted 1994 February 23

ABSTRACT

We report the X-ray spectra of a binary 4U 0614+09 observed with *EXOSAT* on five different occasions in 1984 and 1986. In four observations in 1984, the source intensity was "low" compared to its intensity in the 1986 observation. The source was steady on timescales of 10–1000 s in each of the 1984 observations but highly variable during the 1986 variations. The best-fit spectral models for the continuum are a blackbody spectrum plus an emission from a Comptonized region. In addition, a component due to reflection from a cold disk around the source was needed as an absorbtion edge due to cold or ionized iron was seen near 7 keV with good significance in most of the spectra, particularly in the "low" state. The relation of the hardness ratios with intensity follow the behavior seen in the "Atoll" sources. We have studied the behavior of the hardness ratios with the variations in the parameters of the best-fit spectral models. Most of the variability is associated with the blackbody component thought to arise from the boundary layer on the surface of the neutron star. During the "high" state in 1986, the blackbody temperature is higher, its size smaller, and its contribution significantly greater than in the "low" state. The other notable difference between the two states is the lower opacity in the Comptonized region, and a significantly higher absorption in the "high" state. A weak line emission (equivalent width = 10–40 eV) is detected during the "high" state. The line energy lies between 6 and 7 keV which implies its origin from ionized ion.

Subject headings: binaries: close — stars: individual (4U 0614+09) — X-rays: stars

1. INTRODUCTION

The X-ray source 4U 0614+09 was discovered in the *Uhuru* survey (Giacconi et al. 1974; Forman et al. 1978) and was identified with a blue variable star V1055 Ori which had a *B* magnitude of ~ 18 (Murdin et al. 1974). X-rays from the source have also been detected and studied by Davidsen et al. (1974) (*Copernicus*), Mason et al. (1976) (*Ariel V*), Dower et al. (1978) (*SAS 3*), Swank et al. (1978) (*OSO 8*), Brandt et al. (1992) (*Granat*), and Christian, White, & Swank (1993) (*Einstein Observatory*). It was also observed on several occasions with the *EXOSAT Observatory*.

The source 4U 0614+09 belongs to the class of low-mass X-ray binaries (LMXBs) as it has all the typical characteristics of such objects, viz., temporal variability of the X-ray flux, hardness ratio variations, and occasional X-ray bursts. The *Ariel* sky survey data yielded a periodicity of 5.2 ± 0.3 days which was identified as due to the binary period of the source or a precessing accretion disk (Marshall & Millit 1981). X-ray bursts from 4U 0614+09 were observed by Swank et al. (1978) and Brandt et al. (1992). Optical photometric and spectroscopic observations of V1055 Ori made by Machin et al. (1990), which included a 14 hr simultaneous X-ray monitoring with the *EXOSAT Observatory*, show an anticorrelation between the X-ray and optical fluxes, a behavior that is akin to that of Sco X-1 in certain regimes of X-ray intensity. Like Sco X-1, it also shows X-ray hardness variations correlated with X-ray intensity (Mason et al. 1976; Swank et al. 1978). Optical observations by Machin et al. also found a 10^d periodicity, who ascribed it due precession of an accretion disk. They, however, did not confirm the 5^d periodicity seen in X-rays. The source is at a distance of $\sim 5 \pm 3$ kpc (Swank et al. 1978; Brandt et al. 1992). At that distance its persistent X-ray luminosity is intermediate to the high-luminosity and the low-luminosity LMXBs.

The X-ray spectra of LMXBs generally show two components, a blackbody component and a power-law component or its equivalent emission from a Comptonized region (Sunyaev & Titarchuk 1980). It was suggested that the blackbody component arises from a boundary layer formed by the accretion disk touching the neutron star (White, Stella, & Parmar 1988; Singh, Apparao, & Kraft 1994). The Comptonized component arises when the soft radiation from the inner layers of the accretion disk passes through the hot bloated two-temperature disk or a hot corona around the accretion disk. Low-energy emission-line features due to ionized oxygen and iron, and an absorption edge due to ionized oxygen in the X-ray spectrum of 4U 0614+09 have recently been reported by Christian et al. (1993).

The X-ray spectral variations in LMXBs have been studied using a color-color diagram, which is constructed from ratios of intensities (hardness ratios) in different energy bands, and revealed several patterns of variations in LMXBs (see Hasinger & van der Klis 1989). Of these the "Z-pattern" is well known and seen in most high-luminosity sources, while the other lower luminosity sources exhibit a "banana" shaped band or appear to be confined to "islands"—collectively known as two states of the "Atoll" sources. It is generally believed that these patterns are a result of the variation of the accretion rate $\dot{M}$, and an interaction between the comparatively small magnetic field of the neutron star and the accretion disk. The understanding of these variations, and their correlation with specific components of continuum emission, has remained poor, however.

Here we present, for the first time, a detailed spectral analysis of the *EXOSAT* data on 4U 0614+09 obtained from the archives. We have carried out the analysis with the idea that the high counting rate of the source and its many observations in different intensity states will yield accurate spectral

data which can throw some light on the problems mentioned above.

The paper is organized as follows: We present the data in § 2, analysis and results in § 3, and a discussion in § 4.

2. THE DATA

The source was observed on six different days—4 times in 1984 and twice in 1986, with the X-ray detectors aboard *EXOSAT*. The data were obtained from the *EXOSAT* archives on the final observation tapes (FOTs). The data from the medium-energy (ME) detectors were analyzed. The ME argon-filled (Ar) detectors are sensitive to X-rays in the energy range of 1–20 keV. The details of the detectors are given by Turner, Smith, & Zimmerman (1981). Ar detectors are the best understood of all the *EXOSAT* instruments and have the best signal-to-noise ratios.

The ME data are normally acquired from eight detectors divided into two equal half-arrays. The observations of 4U 0614+09 in 1984 used only one half-array, and the pulse height (PH) data were accumulated using 32 channels. The background data were, therefore, obtained from the other half-array while it was "slewing-in" and "slewing-out" from the source. The observations in 1986 utilized both the arrays by swapping the two halves for the source and background measurements, and the spectral data were available in 64 PH channels. The GSPC data with higher energy resolution but poorer sensitivity were not available in full channel resolution; as a result the energy scale could not be obtained accurately. These data were not analyzed, therefore. The data in the last observation on day 87 of 1986 were contaminated by non–X-ray background and were not analyzed. The details of observations, dates, and times, effective exposure times, and the detected mean count rates in different detectors and energy ranges are given in Table 1. Hereafter, we will refer to the different observations by the year/day number for the start of the observations.

3. ANALYSIS AND RESULTS

3.1. *Temporal Variations: X-Ray Flux and Hardness Ratios*

The data reduction and analysis were performed using the XANADU (X-ray Analysis and Data Utilization) software package. The data were examined for contamination due to non-X-ray events and selected suitably. The mean count rate for 4U 0614+09 showed considerable variations on different days. On shorter timescales of 10 s to a few 1000 s, however, no variations were observed in any given observation during the 1984 observations, i.e., the source was steady during each individual observation in 1984. On the other hand, in 1986 observations, when the source flux was ~3–4 times higher, significant variations were detected on these short timescales. An X-ray light curve obtained from the observation starting in 1986/043 and ending on the next day is shown in Figure 1. The data in the energy range of 1–17 keV have been binned every 100 s and plotted in Figure 1. The contaminated data have been excised at two places showing gaps in the figure. No X-ray bursts were detected in any of the observations.

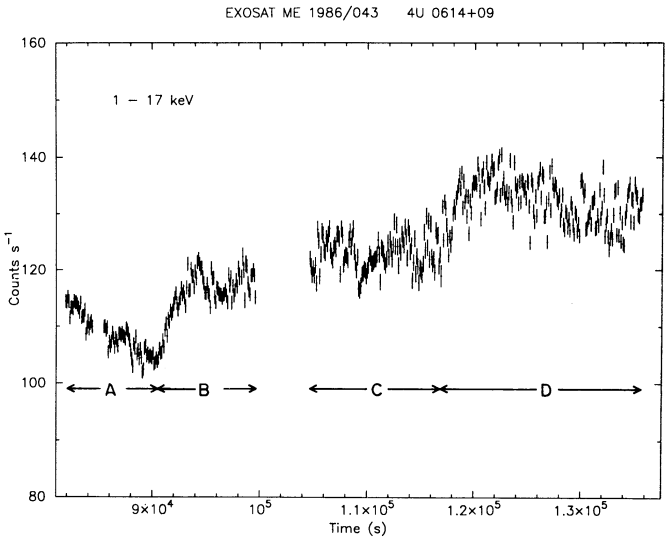

FIG. 1.—X-ray light curve of 4U 0614+09 as observed with the *EXOSAT* ME argon (Ar) detectors on 1986 February 12–13. The data have been binned every 100 s in the energy range of 1–17 keV.

We have determined the hardness ratios HR1 and HR2, defined as (*a*) the ratio of the counts in the 3.2–6 keV energy range divided by counts in the 1–3.2 keV energy range and (*b*) the ratio of the counts in the 6–17 keV energy range divided by counts in the 3.2–6 keV energy range, respectively. In Figure 2, we display the variation in the hardness ratios with the X-ray intensity; the variation of HR1 is shown in the top panel and that of HR2 in the bottom panel. In the 1986 observations, HR1 shows an increasing trend with intensity, whereas a

TABLE 1

DETAILS OF OBSERVATIONS AND COUNT RATES

OBSERVATION START TIME			EFFECTIVE EXPOSURE	DETECTOR	NUMBER OF PH	COUNT RATE[a] 1–20 keV
Year	Day	UT	(s)	HALF	CHANNELS	(10^{-2} cm^{-2} s^{-1})
1984	272	08:01:12	12076	H1	32	8.66 ± 0.016
1984	305	01:45:06	19424	H2	32	8.35 ± 0.015
1984	308	23:17:06	11580	H2	32	6.74 ± 0.015
1984	312	20:34:42	13371	H2	32	6.11 ± 0.020
1986	043	22:37:26	6764	H1[b]	64	20.24 ± 0.026
1986	044	02:37:34	7989	H1[b]	64	21.66 ± 0.025
1986	044	03:47:34	11513	H2	64	22.46 ± 0.017
1986	044	08:39:34	19866	H1[b]	64	23.90 ± 0.017

NOTE.—PH: pulse height corresponding to X-ray energy.

[a] The corresponding PH channels are 1–30 for 1984 data, 1–54 for Half 1 data, and 1–59 for Half 2 data in 1986.

[b] Detector number 3 was off.

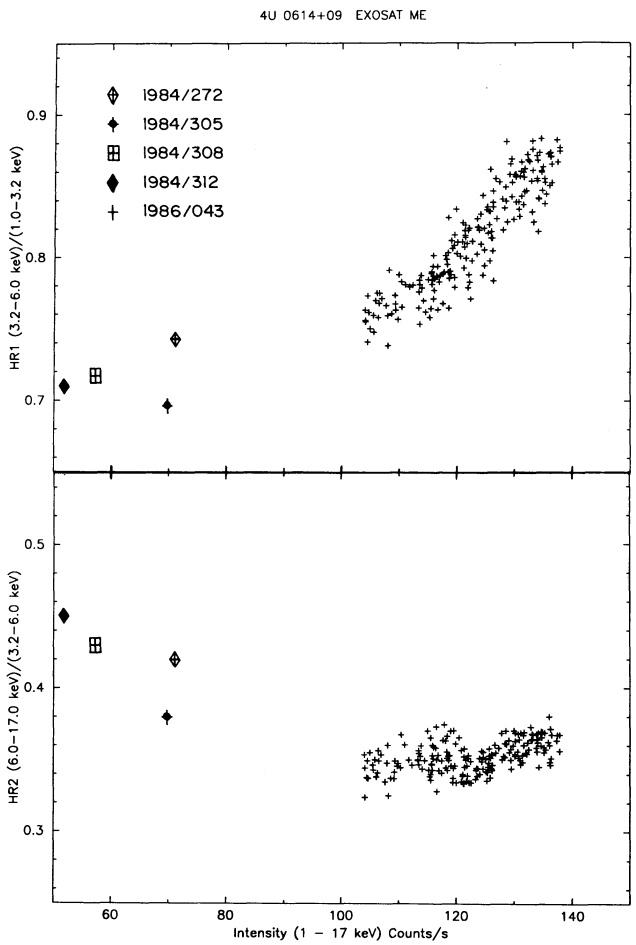

FIG. 2.—Plot of hardness ratios HR1 and HR2, as defined in the text, vs. the X-ray intensity from all observations. The 1986 data have been integrated every 250 s. The 1984 data have been averaged over the entire exposure time of individual observations.

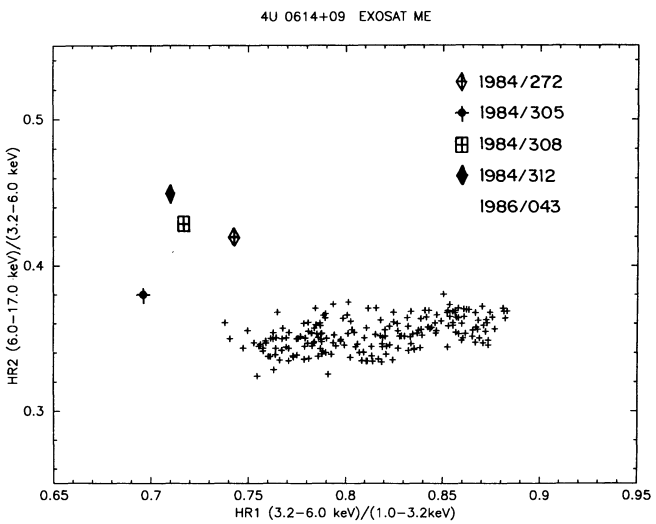

FIG. 3.—Color-color plot of the data using the hardness ratios shown in Fig. 2.

similar trend is not clear in the 1984 observations. The mean value of HR1 is higher in 1986 than in the 1984 observations. On the other hand, HR2 shows a lower mean value and smaller variations in the 1986 observation as compared to the 1984 observations which also show a decreasing trend with intensity. In the color-color diagram shown in Figure 3 we have plotted HR2 versus HR1. In this diagram, the variations of colors resemble the behavior of "Atoll" sources with the 1986 data showing characteristics of a "banana" state and with the 1984 data reminding one of the "island" states where the small scale variations are yet to be discerned with good significance.

3.2. *X-Ray Spectra*

Spectral files were created separately for each observation in 1984. For the 1986 data, since the count rates and the hardness ratios showed significant variations, we accumulated the spectral data in four separate spectral files called A, B, C, and D corresponding to four different periods shown in Figure 1 and listed in Table 1. The "difference" corrections (see White & Peacock 1988) to the PH spectra were applied to the 1986 data and an excellent background subtraction was obtained in all cases. In Figure 4, we show the X-ray spectrum of 4U 0614+09 as observed on two occasions with vastly different intensities viz., 1984/272 and 1986/043C. The spectral shape can be seen to be very different in the two cases representing the 1984 and 1986 data respectively.

The response matrices for the Ar were made using their gain values on the day of the observation. The spectral data were fitted by convolving the input model spectra with the response matrices, and using the χ^2 statistic. In Table 2, we have summarized the minimum χ^2 obtained from various fitted models, for easy comparison as well as for judging the significance of adding different components. *Single-component spectral models*, like a power-law (bare, partially covered or with cold reflection), thermal bremsstrahlung, blackbody, modified blackbody accretion disk models of Shakura & Sunyaev (1973), Stella & Rosner (1984), and Mitsuda et al. (1989), and the Comptonization model of Sunyaev & Titarchuk (1980) (hereafter CompST characterized by electron temperature kT_e and opacity τ) failed to provide an adequate fit to the spectral data and were rejected using the χ^2 statistic. A multiplicative absorption model for low energy X-ray absorption due to intervening medium using cross sections given by Morrison & McCammon (1983) was used throughout. The reduced χ^2, henceforth χ^2_ν, was generally in the range 2–80 (see Table 2, where two single-component models are listed) when any one of these models was used for the data on the objects considered here. An examination of the residuals from single component fit pointed very clearly to the *requirement of at least two continuum components* to improve the χ^2. We adopted a simple blackbody as one of these components, which has been used quite successfully as one of the spectral components present in many low-mass X-ray binaries (see White et al. 1988; Singh et al. 1994). For the second component we again tried all the models mentioned above. We assumed common low-energy absorption for both the components. In all cases, very good fits were obtained when the second component was either a power-law or the CompST model, the two being indistinguishable and equally acceptable based on the χ^2 statistic. Combinations of blackbody with any one of the modified blackbody accretion disk models generally have higher χ^2 values, and were unacceptable for the 1986 data.

In the above analysis we used the PH channels 2–31 for the 1984 data. In the 1986 data, we were forced to ignore a few PH

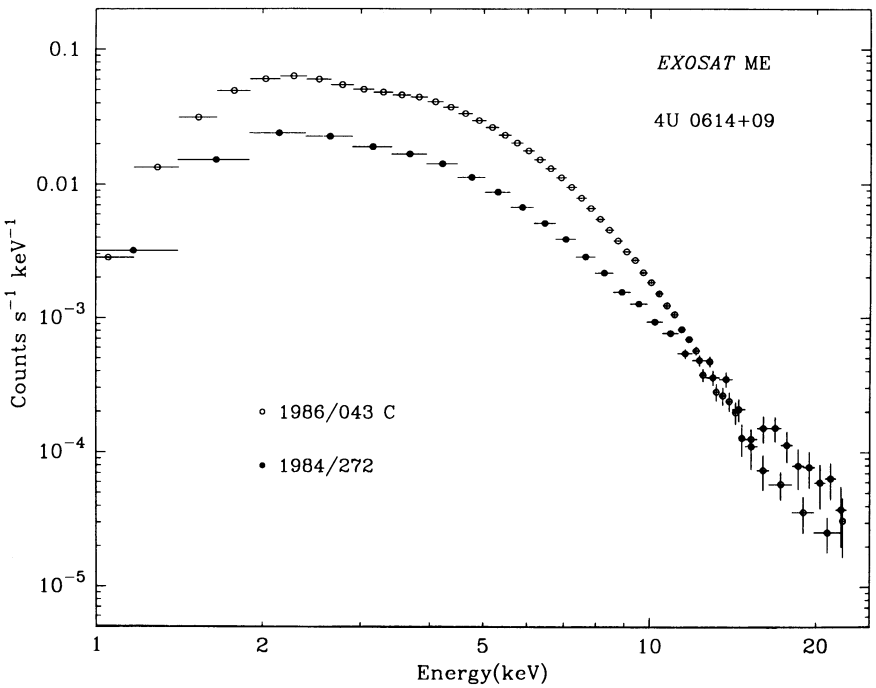

FIG. 4.—The X-ray spectrum of 4U 0614+09 as observed on 1984 September 28 and on 1986 February 13, showing the two different states—"low" in 1984 and "high" in 1986—of the source.

channels between 1.6 and 2.6 keV because of the presence of very sharp residual features whose origin is not understood at present. The first two channels were, however, used throughout as these were very important for estimating the N_H.

The addition of an absorption edge with a maximum depth (τ_m) of $\simeq 0.1$, between 7 and 8.5 keV gave a significant reduction in the minimum χ^2 for five of the eight spectra with $\Delta\chi^2$ in the range of 7.5–14 (see Table 2). Application of the F-statistic implies that the improvements in the χ^2 are significant at better than 99% confidence level in these cases. A similar change in the χ^2 is obtained even when a different set of continuum models is used. The presence of a slightly weaker edge ($\tau_m \leq 0.06$) in the other three spectra cannot be ruled out by statistics.

The addition of a Gaussian with a fixed width ($\sigma = 0.1$ keV), representing line emission, improved the fits significantly only for two of the spectra, viz., 1986/043C ($\Delta\chi^2 = 5$) and 1986/043D ($\Delta\chi^2 = 7$). The equivalent width of the line is in the 10–40 eV range. Therefore, a weak emission line near 7 keV has been detected in two data sets. The best-fit values of the parameters from fitting with a spectral model consisting of a blackbody, CompST, a line feature, an edge, and a common N_H are given in Table 3A. The values derived for the model parameters are displayed along with their allowed ranges with 90% confidence determined using the $\chi^2_{min} + 2.71$ criterion for a single free parameter of interest (Lampton, Margon, & Bowyer 1976).

In Figures 5*a* and 5*b*, we show the residual observed counts after the two-component continuum has been subtracted to display the presence and significance of the edge and line features in the data. The presence of the absorption edges in the spectra prompted us to explore the replacement of one of the

TABLE 2

RESULTS OF SPECTRAL FITTING χ^2_{min}/(Degrees of Freedom) FOR DIFFERENT MODELS

SERIAL NUMBER	SPECTRAL MODELS[a]	OBSERVATION DATE (Year/Day)							
		1984/272	1984/305	1984/312	1984/312	1986/043A	1986/043B	1986/043C	1986/043D
1.	Power Law	41.4/29	58.4/29	72.1/29	106.7/29	1111/54	1562/52	3852/51	4825/56
2.	Comptonization (CompST)[b]	42.5/28	52.0/28	73.4/28	107.9/28	223/53	225/51	129.9/50	388.9/55
3.	Blackbody + Power Law	27.1/26	39.7/26	40.2/26	40.3/26	63.9/51	51.2/49	58.9/48	64.4/53
4.	Blackbody + CompST	27.0/25	40.0/25	40.2/25	34.1/25	64.0/50	51.2/48	59.7/47	64.3/52
5.	Blackbody + CompST + edge	19.4/23	32.5/23	31.6/23	33.1/23	53.1/48	51.2/46	45.8/45	64.3/50
6.	Blackbody + CompST + Gaussian + edge	19.4/21	33.0/21	31.6/21	33.1/21	53.1/46	51.2/46	40.8/43	57.3/52[c]
7.	Blackbody + Cold Reflection	16.3/25	30.6/25[d]	28.8/25	29.0/25	63.1/50	51.2/48	45.8/47	64.9/52
8.	Blackbody + Cold Reflection + Gaussian	16.3/23	30.6/23	28.8/23	29.0/23	63.1/48	51.2/46	41.2/45	57.3/50

[a] A common multiplicative absorbing column is assumed throughout.
[b] Comptonization model based on Sunyaev & Titarchuck 1980.
[c] Without an edge.
[d] Ionized reflector.

TABLE 3A

RESULTS OF SPECTRAL MODELING: BEST-FIT PARAMETER VALUES AND ALLOWED RANGES

	Model Parameters											
		Edge		Blackbody			CompST			Gaussian Line[a]		
Observation (yr/day)	Absorption N_H[b]	Energy (keV)	Maximum Depth	kT (keV)	L[c]	Radius (km)	kT_e (keV)	Optical Depth	Flux[d] (1 keV)	Energy (keV)	Flux[e]	χ^2_{min}/DOF
1984/272	0 (0, 9)	7.5 (6.9, 8.1)	0.10 (0.06, 0.14)	0.67 (0.63, 0.70)	3.5 (3.0, 4.0)	3.7 (3.3, 4.2)	24 (>7)	3.8 (1.5, 7.0)	0.23 (0.22, 0.24)	—	—	19.4/23
1984/305	5 (4, 15)	7.7 (7.2, 8.4)	0.12 (0.07, 0.17)	0.75 (0.69, 0.80)	1.8 (1.6, 2.1)	2.2 (1.9, 2.6)	15 (>7)	4.4 (<7)	0.32 (0.31, 0.33)	—	—	32.5/23
1984/308	0 (0, 10)	7.1 (6.6, 7.6)	0.10 (0.06, 0.14)	0.61 (0.57, 0.62)	3.3 (2.9, 3.9)	4.6 (4.0, 5.0)	14 (7.3, 20)	5.3 (4.5, 7.6)	0.18 (0.17, 0.19)	—	—	31.6/23
1984/312	0 (0, 10)	7.2 (6.2, 8.3)	0.04 (<0.09)	0.56 (0.53, 0.58)	4.0 (3.5, 4.7)	5.7 (5.5, 6.4)	32 (>6.5)	3.6 (1.6, 9.0)	0.14 (0.13, 0.16)	—	—	33.1/23
1986/043A	94 (90, 99)	8.3 (7.9, 8.6)	0.15 (0.11, 0.19)	1.72 (1.70, 1.74)	29.2 (28.8, 29.7)	1.6 (1.5, 1.7)	48 (>10)	1.2 (0.55, 4.0)	2.16 (1.85, 2.45)	—	—	53.1/48
1986/043B	97 (86, 109)	—	—	1.67 (1.65, 1.69)	36.2 (34.2, 38.1)	1.90 (1.8, 2.0)	36 (>7.5)	1.4 (0.5, 3.9)	2.49 (2.19, 2.86)	—	—	51.2/48
1986/043C	91 (82, 101)	7.2 (6.8, 7.6)	0.05 (0.03, 0.06)	1.55 (1.53, 1.57)	32.8 (31.2, 34.5)	2.1 (2.0, 2.2)	29 (>5.9)	1.8 (0.6, 5.4)	2.14 (1.72, 2.33)	6.7 (6.4, 7.1)	4.1 (2.0, 6.3)	40.8/43
1986/043D	44 (35, 53)	—	—	1.58 (1.56, 1.60)	37.6 (36.2, 39.1)	2.16 (2.1, 2.2)	32 (>5)	1.9 (0.7, 6.5)	1.35 (1.10, 1.45)	7.0 (6.7, 7.4)	4.5 (2.3, 6.7)	57.3/50

NOTE.—Allowed ranges are with 90% confidence based on $\chi^2_{min} + 2.71$.

[a] Line width (σ) is fixed at 0.1 keV.

[b] In 10^{20} cm^{-2}.

[c] Luminosity in 10^{35} ergs s^{-1}; distance = 5 kpc.

[d] Photons cm^{-2} s^{-1} keV^{-1}.

[e] 10^{-4} photons cm^{-2} s^{-1}.

TABLE 3B

RESULTS OF SPECTRAL MODELING: BEST-FIT PARAMETER VALUES AND ALLOWED RANGES

	Model Parameters										
		Blackbody			Power Law and Reflection[a]			Gaussian Line[b]			
Observation (yr/day)	Absorption N_H[c]	kT (keV)	L[d]	Radius (km)	Γ[e]	Ω[f]	Flux[g] (1 keV)	Energy (keV)	Flux[h]	χ^2_{min}/DOF
1984/272	16 (3.5, 30)	0.77 (0.74, 0.80)	3.2 (2.1, 4.2)	2.6 (2.1, 3.1)	2.11 (2.04, 2.19)	2 (>1.6)	0.314 (0.311, 0.317)	—	—	16.3/25
1984/305	20 (9, 29)	0.94 (0.87, 1.06)	2.3 (1.7, 3.0)	1.5 (1.1, 2.0)	2.27 (2.21, 2.33)	1.6 (>0.4)	0.39 (0.36, 0.42)	—	—	33.8/25
1984/308	16 (2, 29)	0.69 (0.64, 0.73)	2.6 (1.7, 3.5)	3.0 (2.5, 3.5)	2.1 (2.0, 2.2)	2 (>1.2)	0.24 (0.20, 0.29)	—	—	28.8/25
1984/312	1 (1, 20)	0.62 (0.57, 0.64)	3.8 (2.9, 4.4)	4.5 (3.9, 5.2)	1.92 (1.85, 2.04)	2 (>1.3)	0.16 (0.14, 0.19)	—	—	29/25
1986/043A	110 (98, 122)	1.64 (1.62, 1.66)	31.5 (29.5, 33.5)	1.84 (1.77, 1.91)	3.27 (3.14, 3.40)	1.0 (>0.1)	2.70 (2.3, 3.2)	—	—	63.1/50
1986/043B	98 (87, 109)	1.67 (1.65, 1.68)	36.2 (34.2, 38.0)	1.90 (1.8, 2.0)	3.2 (3.1, 3.3)	0 (<1.1)	2.58 (2.22, 2.90)	—	—	51.2/48
1986/043C	98 (89, 107)	1.51 (1.49, 1.53)	32.8 (31.5, 34.3)	2.22 (2.17, 2.27)	3.1 (3.0, 3.2)	1.2 (0.25, 2.0)	2.38 (2.14, 2.67)	6.6 (6.25, 6.9)	4.0 (1.9, 6.2)	41.2/45
1986/043D	45 (36, 55)	1.58 (1.56, 1.60)	37.7 (36.2, 39.2)	2.17 (2.12, 2.2)	2.7 (2.6, 2.8)	0 (<0.7)	1.38 (1.25, 1.55)	7.0 (6.7, 7.4)	4.6 (2.3, 6.8)	57.3/50

NOTE.—Allowed ranges are with 90% confidence based on $\chi^2_{min} + 2.71$.

[a] Escaping fraction of the power law is 1 (isotropic source), and inclination of the disk is zero.

[b] Line width (σ) is fixed at 0.1 keV.

[c] In 10^{20} cm^{-2}.

[d] Luminosity in 10^{35} ergs s^{-1}; distance = 5 kpc.

[e] Photon index.

[f] Solid angle subtended by the disk/2π.

[g] Photons cm^{-2} s^{-1} keV^{-1}.

[h] 10^{-4} Photons cm^{-2} s^{-1}.

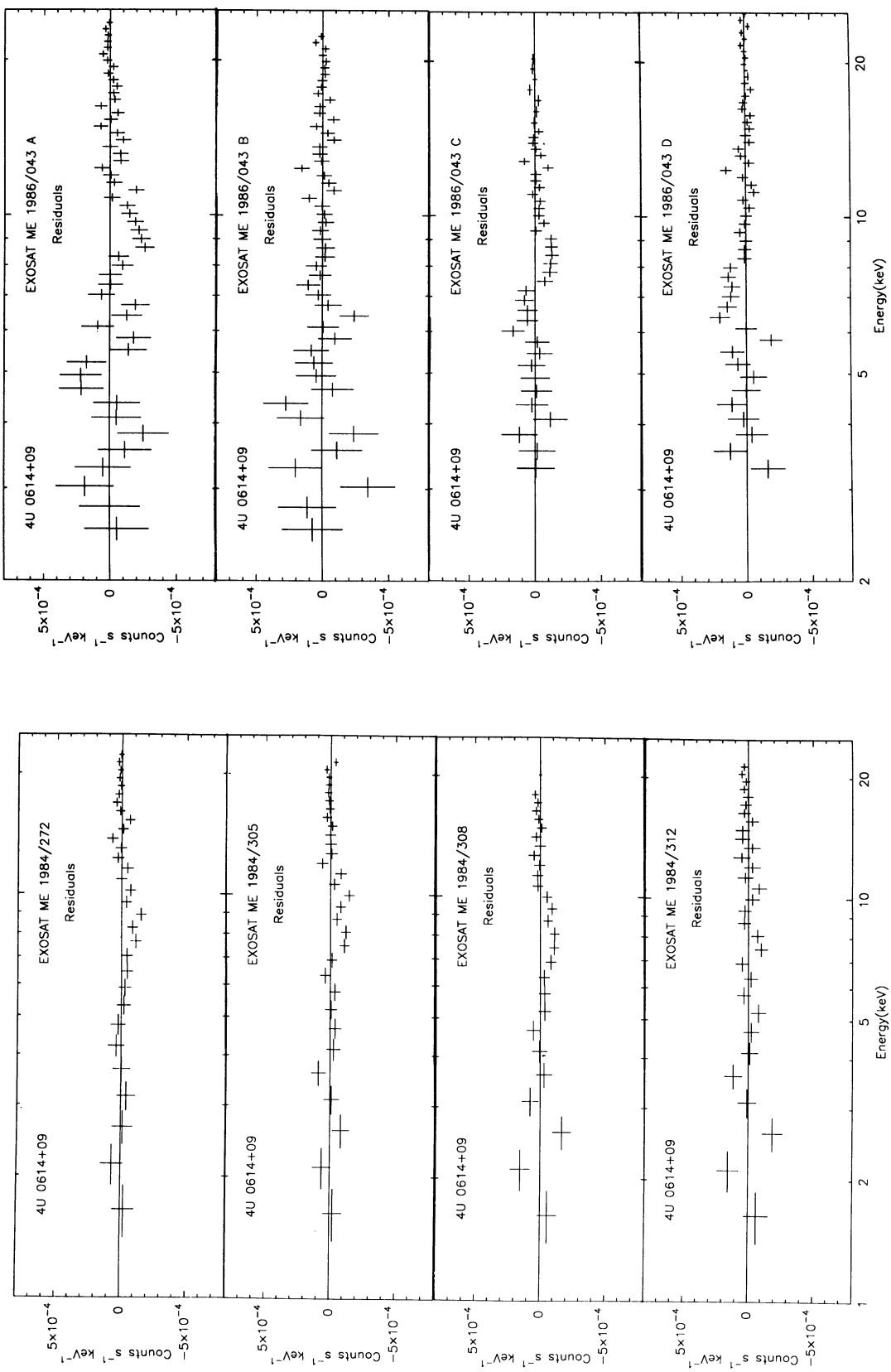

FIG. 5a

FIG. 5b

FIG. 5.—Residuals after subtracting the best-fit continuum models: (*a*) 1984 data, and (*b*) 1986 data. The presence of an edge can be seen in five of the spectra and a weak narrow Gaussian line in two of the spectra.

continuum components viz., CompST, by a power law plus its reflection from a cold matter or ionized matter in a disk around the source as calculated by Lightman & White (1988). The spectral parameters of this model are (*a*) photon index of the intrinsic, illuminating power law; (*b*) fraction of power law escaping toward the observer (frozen to unity here, implying an isotropic X-ray source); (*c*) inclination of the disk to the observer (fixed at zero degrees due to lack of any dependence during the spectral fitting); (*d*) solid angle subtended by the disk; and (*e*) the maximum energy extent of the power law (fixed at 300 keV). For an ionized reflector the ionization parameter and the temperature of the disk are additional parameters (see Done et al. 1992). In all spectra except the one on 1986/043A, equally good or slightly better fits were obtained with the choice of an isotropic power law source plus reflection from a disk with zero inclination. The presence of absorption edges due to reflection is an inherent feature of this model. Line emission which is very weak and present at the most in two spectra (see above), still needed to be accounted for by being modeled separately as a Gaussian. The best-fit values and the allowed ranges of the parameters of these models are listed in Table 3B. The best-fit model constrains the solid angle subtended by the disk to some extent. In one of the spectra, viz., 1984/305, an ionized reflector was a somewhat better fit ($\Delta\chi^2 = 3.7$) than a cold reflector with an ionization parameter of ~ 10 and disk temperature of $\sim 10^7$ K. For the rest, the two types gave identical χ^2.

The deconvolved X-ray spectra are shown for two of the observations, viz., 1984/272 and 1986/043C in Figures 6 and 7, respectively. The contribution of the different components is shown separately to show how these components change as the source moves from a "low" state to a "high" state.

4. DISCUSSION

4.1. *X-Ray Continuum*

The *EXOSAT* observations of 4U 0614+09 show that the source was in a higher X-ray intensity state in 1986 than in 1984. The total X-ray luminosity in the "high" state was in the range (8–10) $\times 10^{36}$ ergs s^{-1} as compared to (3–4) $\times 10^{36}$ ergs s^{-1} in the "low" state, for an assumed distance of 5 kpc. In both the states, the X-ray continuum is best fitted by either of the following two models: (*a*) blackbody plus emission from a Comptonized cloud and a common low-energy absorption or (*b*) blackbody plus a power law and its reflection from a cold or ionized matter. The presence of edges between 7 and 8 keV in the spectra, irrespective of the continuum model used, favor the second option somewhat. A power law is also a simple approximation to the emission from a Comptonized cloud with fewer parameters; however, the best-fit values obtained from fitting the Comptonized component give a better physical insight to the source of emission, in which case, the presence of the edges in the X-ray spectra just shows the reflection of the Comptonized component by the disk.

The "high" and the "low" states show significant differences in their spectra which are summarized in Table 4. The most notable difference is the change in the parameters of the best-fit blackbody. In the "high" state, the blackbody luminosity increases by an order of magnitude contributing over one-third of the total luminosity, up from about one-tenth in the "low" state. In contrast, the luminosity of the Comptonized component increases by a factor of two only. The Comptonization parameter, $y = 4kT_e\tau^2/m_e c^2$, decreased by a factor of ~ 4 in the "high" state reflecting its lower opacity. It is interesting to see that while the temperature of the black-

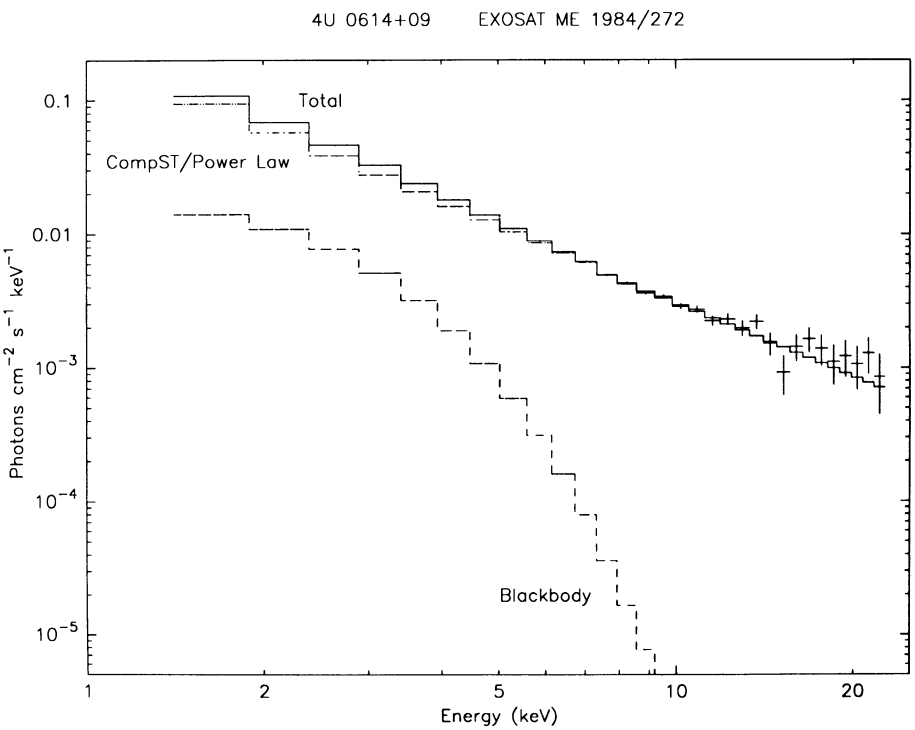

FIG. 6.—Deconvolved best-fit spectrum from the 1984/272 observation. Different components are shown separately and have been marked in the figure.

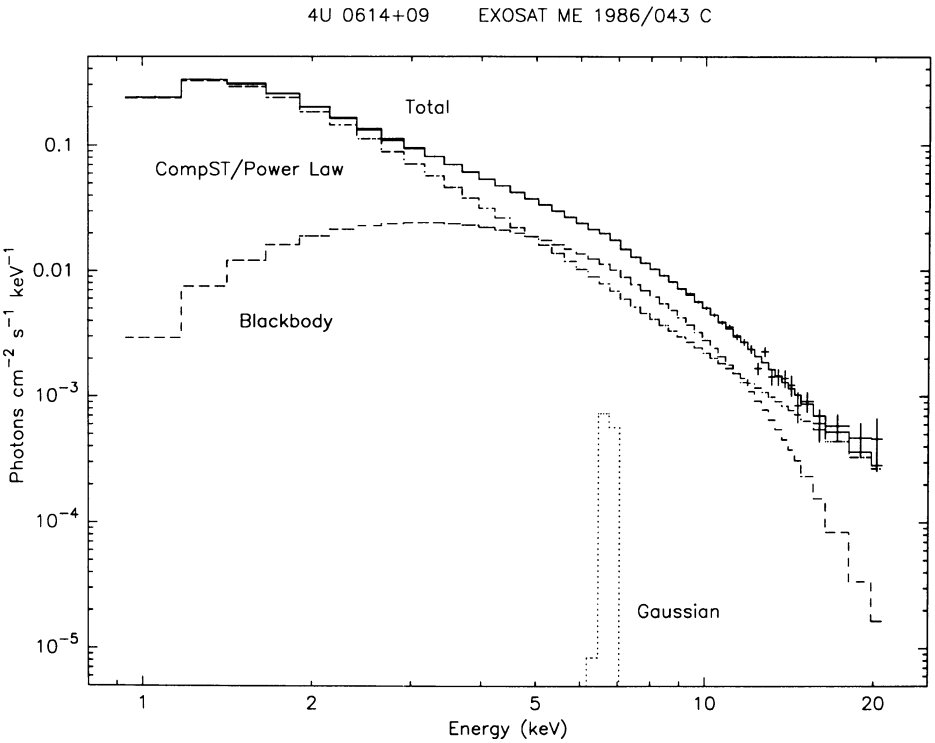

FIG. 7.—Deconvolved best-fit spectrum from the 1986/043C observation. Different components are shown separately and have been marked in the figure.

body goes up by factor of ~3, the spherical radius of its projected area becomes smaller in the "high" state than in the "low" state. These variations are shown in Figure 8 as a function of the total luminosity which depends on the accretion rate.

We have interpreted earlier (Singh et al. 1994), along with White et al. (1988), that the blackbody component is due to a boundary layer where the accretion disk meets the surface of the neutron star. The area of the blackbody-emitting region derived here is consistent with this interpretation. This boundary layer for an accreting neutron star is, however, not studied in detail even though calculations have been made for accreting white dwarfs (Narayan & Popham 1993). Our observations of the characteristics of the boundary layer, viz., the dependence of the temperature and area of the blackbody on the total X-ray luminosity or the accretion rate, place constraints on such calculations.

The higher luminosity of the Comptonized component when the source is in the "high" state can be expected due to the passage of the increased soft flux from a hotter blackbody through the hot gas of a two-temperature accretion disk suggested (White et al. 1988; Singh et al. 1994) to have formed as the accretion disk approaches closer to the neutron star surface for higher accretion rates. The behavior of the Comptonization

TABLE 4

DIFFERENCES IN THE TWO STATES OF 4U 0614+09

Parameter	"Low" State	"High" State
Total luminosity[a,b]	3–4 × 10^{36}	8–10 × 10^{36}
Variability amplitude	Small	Large
Variability timescale	Days	Minutes-to-hours
Color characteristics	"Island" State	"Banana" State
Blackbody luminosity[b]	1.8–3.4 × 10^{35}	≃30 × 10^{35}
Blackbody radius[b,c]	2–6 km	1.5–2.2 km
Blackbody temperature	≃0.6 keV	≃1.6 keV
Blackbody fraction	5%–12%	≃35%
Optical depth (Comptonized region)	~4	~1.5
Comptonization parameter (y)	≃2.8	≃0.7
Flux at 1 keV (CompST)[d]	≃0.2	≃2
Low energy absorption[e]	≤10^{21}	≃10^{22}
Line emission	Not detected	Detected
Solid angle of reflector	>2π	≤2π

[a] Units: ergs s^{-1} (1–20 keV bandwidth; not corrected for absorption).
[b] Distance = 5 kpc.
[c] Assuming a spherical shape for the projected area.
[d] Units: photons cm^{-2} s^{-1} keV^{-1}.
[e] Equivalent column of N_H in cm^{-2}.

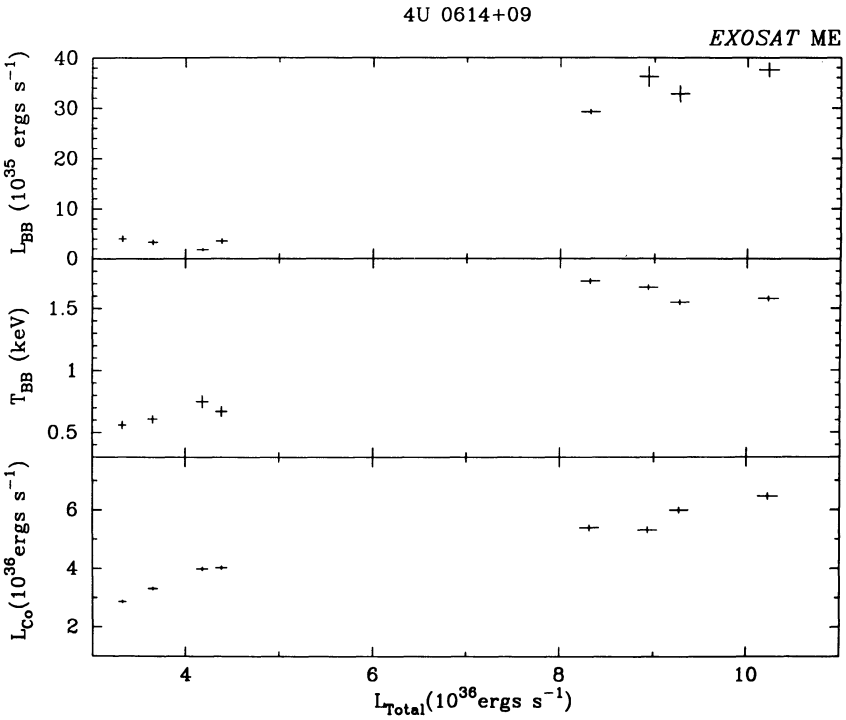

FIG. 8.—Variation of the blackbody luminosity, blackbody temperature, and luminosity of the Comptonized cloud is shown as a function of the total luminosity and hence the accretion rate.

parameter is similar to that found in 4U 1957+11 and consistent with the earlier explanation based on a two-temperature disk (Singh et al. 1994).

4.2. *Low-Energy Absorption, Edges, and Reflection*

The low-energy absorption in the X-ray spectrum during the "low" state, $\simeq 10^{21}$ cm^{-2}, is consistent with the reddening due to the interstellar matter in the direction of the source, thereby implying negligible absorption in the source. On the other hand, in the "high" state the source exhibits significantly higher absorption $(5–10) \times 10^{21}$ cm^{-2}. This additional absorption could be due to a wind from the hot inner disk, suggested by Apparao & Tarafdar (1993). Absorption edges are detected between 7 and 8 keV and are most probably due to cold or ionized iron (Fe I to Fe XXII). The maximum depth of the absorption edge τ_m ($\simeq 0.1$) can be used to estimate the column density of the absorbing iron. Using the photoelectric absorption cross section of 3.8×10^{-20} cm^2 atom^{-1} for Fe I we derive a value of 2.6×10^{18} cm^{-2} for the column density of Fe I. For a value of 3.3×10^{-5} for the abundance of iron, the equivalent column density of absorbing matter (N_H) is 8×10^{22} cm^{-2} which is at least 8 times higher than seen in the low-energy absorption indicating an overabundance of iron or special geometrical conditions. A plausible geometry is described below: the direct component (power-law or CompST) visible to the observer passes through an edge of the accretion disk and leads to low-energy absorption. The Fe absorption edges are imprinted on the spectrum due to reflection by cold or partially ionized material which is not in the same line of sight and, therefore, lead to an estimate of N_H which is different from the value obtained from low-energy absorption. It is also possible that the low-energy absorption varies due to a possible precession of the disk which modulates the matter in the line of sight without seriously affecting the reflected portion of the spectrum.

Line emissions in the high state and/or strong, rapid variability in the high state may reduce the depth of the absorption edge in the spectrum, thus making it difficult to observe the edge.

4.3. *Line Emission*

Line emission is seen only in the "high" state of the source after it has nearly reached the maximum brightness. The equivalent width of the line is measured to be 10–40 eV, which is very small. Even though the relative number of photons with energies greater than 6 keV declined in the "high" state (see HR2 in Fig. 2), there is an increase in the absolute number of photons above 6 keV due to higher intensity which could have boosted the line emission to detectable levels. We would, however, like to caution that the lack of full energy channel resolution (32 instead of 64) in the "low" state can also be responsible for the nondetection of weak line emission in the "low" state. The energy of the line indicates emission from iron, in a cold or ionizated state, through collisional excitation or recombination in a photoionized region. Many sites for the origin of line emission have been pointed out by Kallman (1989) who also calculated that the accretion disk corona has the appropriate conditions to produce the iron K-line in a photoionized region. The absorption edges can also be produced in the corona, and be detected when we view an inclined disk, as demonstrated by Vritlek, Soker, & Raymond (1993).

5. CONCLUSIONS

The X-ray spectral study of 4U 0614+09 shows that its spectrum is similar to that of other LMXBs (see White et al.

1988; Singh et al. 1994). Blackbody emission component is detected in all observations along with a Comptonized component. It is the most variable component in the source. The variations in its spectral hardness resemble those found in the class of sources known as "Atoll" sources. An absorption edge due to cold or ionized iron is detected in its X-ray spectra and indicates reflection from a cold or ionized disk. Line emission due to iron is detected in its "high" state. Observations with broad-band instruments with energy range of 1–100 keV are needed to understand the complex nature of spectral variations in the source. This will also allow the construction of more useful color or hardness ratio diagrams in which the blackbody and CompST (or power-law) components are clearly separable.

The XANADU software package for the SUN Unix system was provided by A. Tennant of the Marshall Space Flight Center, and XSPEC Version 8.33 used for spectral fitting was acquired from the High Energy Astrophysics Science Archive Research Center at the Goddard Space Flight Center.

REFERENCES

Apparao, K. M. V., & Tarafdar, S. P. 1993, J. Astrophys. Astron., 14, 135
Brandt, S., Castro-Tirado, A. J., Lund, N., Dremin, V., Lapshov, I., & Sunyaev, R. 1992, A&A, 262, L15
Christian, D. J., White, N. E., & Swank, J. 1993, preprint
Davidsen, A., et al. 1974, ApJ, 193, L25
Done, C., Mulchaey, J. S., Mushotzky, R. F., & Arnaud, K. A. 1992, ApJ, 395, 275
Dower, R. G., et al. 1978, Nature, 273, 364
Forman, W., et al. 1978, ApJS, 38, 357
Giacconi, R., et al. 1974, ApJS, 27, 37
Hasinger, G., & van der Klis, M. 1989, A&A, 225, 79
Kallman, T. R. 1989, Proc. 23d ESLAB Symposium: Two Topics in X-Ray Astronomy 1. X-Ray Binaries, ed. J. Hunt & B. Battrick (ESA SP-236) 1, 157
Lampton, M., Margon, B., & Bowyer, S. 1976, ApJ, 208, 177
Lightman, A. P., & White, T. R. 1988, ApJ, 335, 57
Machin, G., et al. 1990, MNRAS, 247, 205
Marshall, N., & Millit, J. M. 1981, Nature, 293, 379
Mason, K. U., et al. 1976, MNRAS, 177, 513
Mitsuda, K., Inoue, H., Nakamura, N., & Tanaka, Y. 1989, PASJ, 41, 97
Morrison, R., & McCammon, D. 1983, ApJ, 270, 119
Murdin, P., et al. 1974, MNRAS, 169, 25
Narayan, R., & Popham, R. 1993, Nature, 362, 820
Shakura, N. I., & Sunyaev, R. A. 1973, A&A, 24, 337
Singh, K. P., Apparao, K. M. V., & Kraft, R. 1994, ApJ, 421, 753
Stella, L., & Rosner, R. 1984, ApJ, 277, 312
Sunyaev, R. A., & Titarchuk, L. G. 1980, A&A, 86, 121
Swank, J. H., Becker, R. H., Boldt, E. A., Holt, S. S., & Serlemitsos, P. J. 1978, MNRAS, 182, 349
Turner, M. J. L., Smith, A., & Zimmerman, H. U. 1981, Space Sci. Rev., 30, 513
Vrtilek, S. D., Soker, N., & Raymond, J. C. 1993, ApJ, 404, 696
White, N. E., & Peacock, A. 1988, Mem. Soc. Astr. Italiana, 59, 7
White, N. E., Stella, L., & Parmar, A. N. 1988, ApJ, 324, 363